

## In-Orbit Attitude Performance of the 3-Axis Stabilised SNAP-1 Nanosatellite

Dr.W.H. Steyn and Y. Hashida

Surrey Space Centre

University of Surrey, Guildford, England

Tel: +44(0)1483 689278, e-mail: [h.steyn@sstl.co.uk](mailto:h.steyn@sstl.co.uk), [y.hashida@sstl.co.uk](mailto:y.hashida@sstl.co.uk)

**Abstract.** SNAP-1 is the first 3-axis stabilised nanosatellite in orbit. The satellite is stabilised by a single Y-momentum wheel and 3-axis magnetorquer rods, used for nutation damping and wheel momentum management. The primary attitude sensor used for attitude and rate estimation, is a miniature 3-axis magnetometer. This paper will show the attitude performance results during pointing of the CMOS cameras. One of the challenges was how to handle a large residual magnetic moment disturbance on the satellite. This disturbance was caused by an unforeseen permanent magnetisation dipole from the thruster solenoids, which could not be fully cancelled by the magnetorquer rods. To enable the onboard attitude and rate Kalman filter to give accurate state estimates, the magnetic disturbance was first characterised and then partially compensated for, using the magnetorquer rods. The paper will explain how this problem was solved, before the Y-momentum wheel could be utilised to stabilise and point the imaging payload. The attitude disturbances during firings of the butane gas thruster will also be presented and characterised. The effect of these firings on the orbit will be shown as measured by the GPS receiver on SNAP-1. The lessons learned from the AODCS design of a SSTL nanosatellite are summarised.

### Introduction

The 6.5 kg nanosatellite SNAP-1 (Surrey Nanosatellite Applications Platform) was launched on the 28<sup>th</sup> of June 2000 with the Tsinghua-1 microsatellite on a Cosmos launch into a 704 km sun-synchronous circular orbit. One of the ADCS objectives<sup>1</sup> was to demonstrate 3-axis stabilisation during nominal nadir viewing for earth imaging. Another was to demonstrate a propulsion system<sup>2</sup> and formation flying with Tsinghua-1.

The attitude and orbit control system design has already been reported at the 2000 USU conference<sup>1</sup>. The SNAP-1 actuator and sensor specifications are summarised in Table 1. Figure 1 is a photograph of the AODCS hardware (excluding the propulsion system).

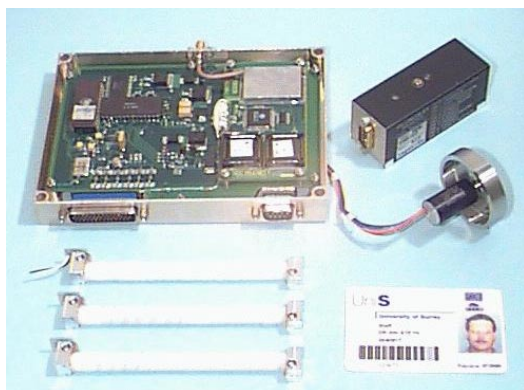


**Figure 1:** AODCS Hardware

After launcher separation SNAP-1 had a 5 rpm tumble rate. After activation of a magnetorquer rate damping controller, the initial high rate was damped within 1 day to zero values in the X and Z-body axes. The Y-rate was damped to about 2 rotations per orbit with a somewhat surprising result, i.e. the space pointing facet (-Z axis) was almost perfectly tracking the local geomagnetic field vector (B-field). Although the magnetic controller was designed to put the satellite into a Y-Thomson spin, it was suppose to track a constant Y-spin rate reference of 10 rotations per orbit. The compass mode attitude response was then attributed to an internal unmodelled magnetic moment almost aligned with the spacecraft's Z-axis.

The source of the disturbance was eventually traced to magnetic remanence in the dual solenoid valves of the propulsion thruster. The 2 solenoids were supposed to have been wired in opposite polarities, but somehow it never happened. So, instead of having residual magnetic moments that cancel, the 2 dipole moments were summed, resulting in a fairly large magnetic disturbance.

The first step was to quantify the magnitude and direction of the disturbance magnetic moment and then, if possible, to use the magnetorquer rods to generate a cancellation moment.

**Table 1:** ADCS Sensor and Actuator Specifications

|                                 | Magnetometer             | GPS                      | Torqrod                  | Momentum wheel           | ADCS Module               |
|---------------------------------|--------------------------|--------------------------|--------------------------|--------------------------|---------------------------|
| <b>Manufacturer</b>             | Billingsley              | SSTL                     | SSTL                     | SSTL                     | SSTL                      |
| <b>Quantity</b>                 | 1                        | 1                        | 3                        | 1                        | 1                         |
| <b>Type</b>                     | Fluxgate                 | Mitel Chipset            | Nickel-alloy core        | Brushless DC Motor       | C515 CAN $\mu$ Controller |
| <b>Range</b>                    | $\pm 60 \mu\text{Tesla}$ | 12-Channel<br>1-Antennae | $\pm 0.127 \text{ Am}^2$ | 0-5000 rpm<br>0-0.01 Nms | -                         |
| <b>Resolution/<br/>Accuracy</b> | $\pm 60 \text{ nT}$      | < 15 meter               | 10 msec min.<br>pulse    | $\pm 5 \text{ rpm}$      | -                         |
| <b>Mass (gram)</b>              | 117                      | 43                       | 36 each                  | 80                       | 300                       |
| <b>Size (mm)</b>                | 35x32x83                 | 95x50x8                  | 125x $\Phi$ 5            | 40x $\Phi$ 47            | 168x122x20                |
| <b>Power (mW)</b>               | 150                      | 1700                     | 100                      | 100-500                  | 250                       |

### Initial Performance

Figure 2 shows a typical B-field measurement onboard SNAP-1 during compass mode. It is clear from this figure that the negative Z-axis is roughly aligned to the B-field vector  $\mathbf{B}$ . The direction of the disturbance magnetic moment will try to align itself to  $\mathbf{B}$  in body coordinates, similar to a compass needle tracking the B-field lines. Therefore by determining the average direction over many orbits of the measured  $\mathbf{B}$  vector in the body coordinates, the direction of the body fixed internal disturbance magnetic moment vector  $\mathbf{M}_d$  will be known. Table 2 shows the average B-field body components over a 24 hour period during compass mode.

**Table 2:** Average Magnetometer Measurements

| $B_x\text{-average}$ | $B_y\text{-average}$ | $B_z\text{-average}$ |
|----------------------|----------------------|----------------------|
| 5.2 $\mu\text{T}$    | 10.1 $\mu\text{T}$   | -29.9 $\mu\text{T}$  |

From this the azimuth and elevation angles of  $\mathbf{M}_d$  can be calculated as: Azimuth  $\alpha = 62.8^\circ$  and Elevation  $\beta = -69.2^\circ$ . The magnitude of the magnetic moment disturbance can be calculated by using a simplified dynamic model for the  $B_x$  and  $B_z$  oscillations seen in Figure 2. Assuming a restoring magnetic torque when the magnetic moment vector and the magnetic field vector are misaligned by an angle  $\theta$ , the following model can be used:

$$I\ddot{\theta} = N_d = -\|\mathbf{B}_{avg}\| \|\mathbf{M}_d\| \sin \theta \quad (1)$$

with,

$I$  = MOI of the satellite

$\|\mathbf{B}_{avg}\|$  = Average B-field magnitude

Using a small angle assumption, the model above is that of a classical oscillator with frequency:

$$\omega_d = \sqrt{\|\mathbf{B}_{avg}\| \|\mathbf{M}_d\| / I} \quad (2)$$

From Figure 2 we have roughly 10 oscillations per orbit. Thus  $\omega_d = 0.0106 \text{ rad/s}$ ,  $I = 0.058 \text{ kgm}^2$  and  $\|\mathbf{B}_{avg}\| = 32.5 \mu\text{T}$ . This gives  $\|\mathbf{M}_d\| = 0.2 \text{ Am}^2$ , or in vector form using the azimuth and elevation angles: (3/8/2000)

$$\mathbf{M}_d = [0.033 \quad 0.063 \quad -0.187]^T \text{ Am}^2 \quad (3)$$

The first step towards 3-axis stabilisation was to enable the Y-momentum wheel to prevent the satellite body from rotating around the B-field vector in compass mode (prevent large yaw rotations). The Y-wheel was commanded to -1000 rpm (-0.002 Nms) with the spin axis roughly normal to the orbit plane. After damping of the Y-body rate the satellite body settled into a compass mode attitude again. The magnetic disturbance was recalculated (using the simple procedure above) after some thruster firings with the Y-wheel running and the result this time (2 months later) was: (3/10/2000)

$$\mathbf{M}_d = [0.034 \quad 0.042 \quad -0.165]^T \text{ Am}^2 \quad (4)$$

The magnitude was noticed to be slightly less and there was a small directional change as well. The next step was to use the magnetorquer rods to cancel the disturbance moment. It can be observed that the  $M_z$  component is larger than the maximum torquer rod moment of  $0.127 \text{ Am}^2$ . Furthermore when a 5 second ADCS sampling period is used, the maximum on-pulse is only 4 seconds for the torquer rods. This is to have a window of 1 second wherein an undisturbed magnetometer measurement can be sampled. The effective Z-torquer moment for 4 second pulses will then be only  $0.1 \text{ Am}^2$ . With this torquer firing (80% of the time) and the Y-wheel running at -2000 rpm, the procedure above was repeated to determine the residual  $\mathbf{M}_{d-res}$ . This gave  $\|\mathbf{M}_{d-res}\| = 0.05 \text{ Am}^2$  and also a significant change in the direction:

(17/11/2000)

$$\mathbf{M}_{d-res} = [0.041 \quad 0.015 \quad -0.023]^T \text{ Am}^2 \quad (5)$$

The final step was to compensate fully for the X and Y-axis disturbance moment by firing the corresponding torquer rods. The compensation magnetic moment delivered by magnetorquer rods was:

$$\mathbf{M}_{MT} = [-0.041 \quad -0.015 \quad 0.1]^T \text{ Am}^2 \quad (6)$$

Ideally this will leave the satellite with only a small disturbance moment in the Z-axis of  $M_{dz} = -0.023 \text{ Am}^2$ . The magnetic disturbance torque can then be calculated as:

$$\mathbf{N}_d = \mathbf{M}_{eff} \times \mathbf{B} = [-B_y M_{dz} \quad B_x M_{dz} \quad 0]^T \quad (7)$$

with,

$\mathbf{B}$  = Body measured B-field

For a polar orbit and a Y-momentum stabilised satellite (small roll and yaw angles) the  $B_y$  component of the B-field will be very small, resulting in a small magnetic disturbance in the X-axis, see (7). The Y-axis magnetic disturbance can be significant over the equatorial regions, with  $B_x$  large for a nadir pointing attitude. Fortunately, the Y-wheel pitch attitude controller will be able to do disturbance rejection in the Y-axis. This controller was designed<sup>2</sup> to have a fast 2% settling time of 2 minutes.

Figure 3 shows the 3-axis stabilisation performance over a 28 hour period with the magnetorquer

compensation values of (6). Additionally the magnetorquers were also used to damp out any roll and yaw nutation and to maintain the wheel at a constant momentum. The Y-momentum wheel was also used to implement the pitch control, as discussed. Although SNAP-1 could be kept roughly nadir pointing without any difficulty, the roll and yaw attitude performance was still not satisfactory: e.g. roll  $1-\sigma$  variation =  $11.2^\circ$ , see Table 5 for a summary of the performance results. The wheel momentum could be maintained close to a speed of  $-2700 \text{ rpm}$  (see Figure 4) and the  $\pm 300 \text{ rpm}$  variation once per orbit was needed to compensate for the residual magnetic disturbance torque in the Y-axis (7).

In an attempt to improve the accuracy of the disturbance magnetic moment compensation, it was decided to develop a proper magnetic disturbance estimator. The simple technique presented in this paragraph have the following limitations:

- It does not take the full satellite dynamics into account (wheel, gyroscopic torques etc.)
- It assumes ideal magnetorquer compensation (no cross coupling effects)
- It does not track changes in the disturbance magnetic moment.

The disturbance estimator will be discussed in the next paragraph.

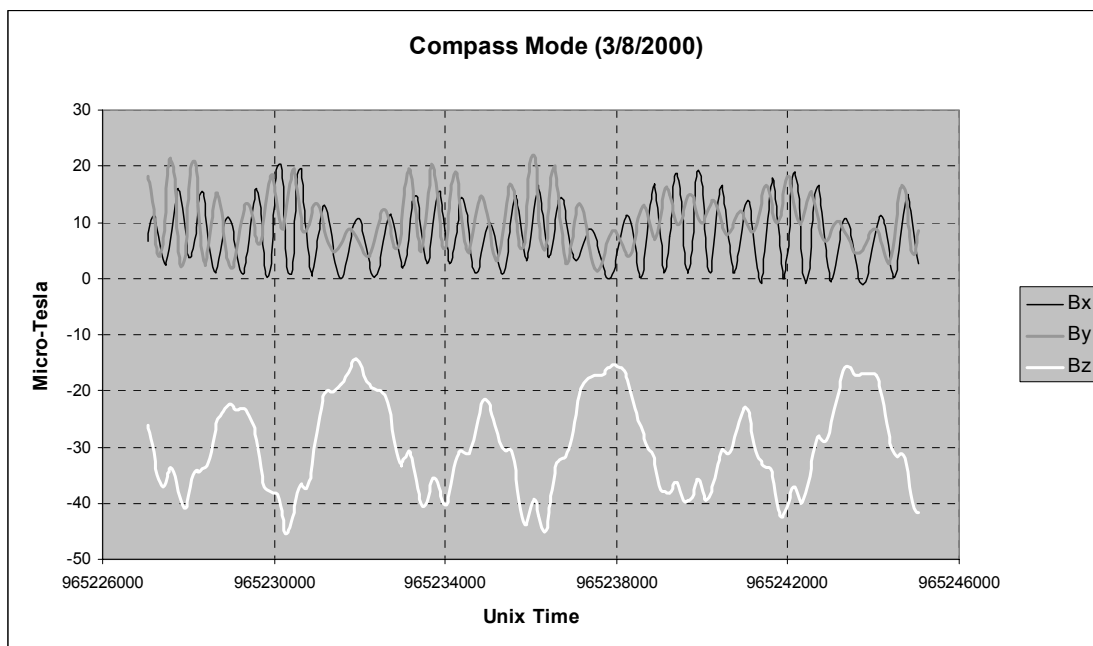


Figure 2: B-field measurement during Compass Mode tracking

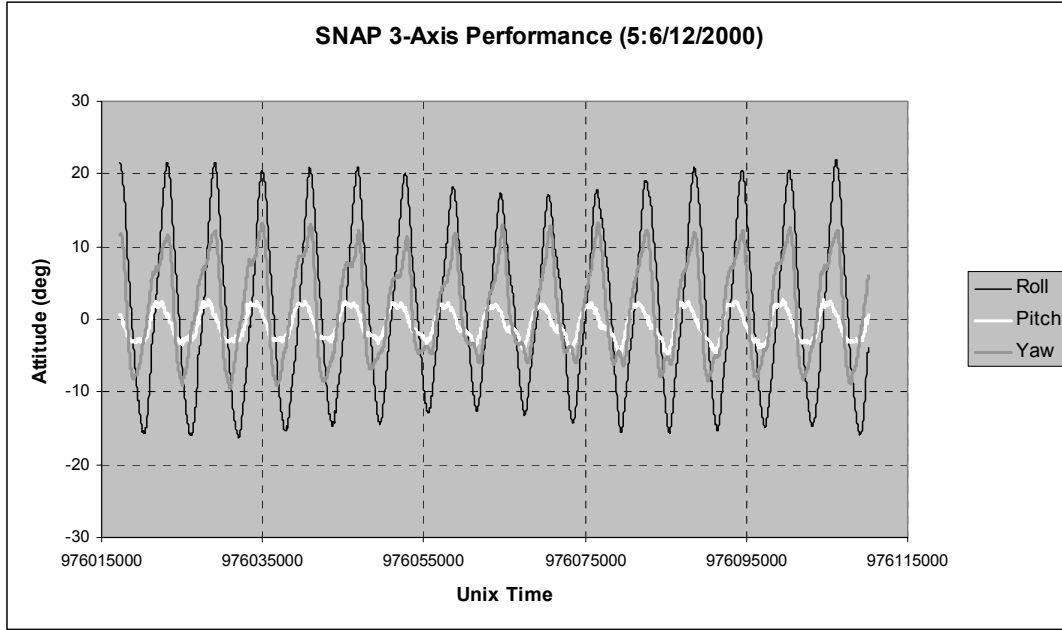


Figure 3: Initial 3-Axis performance with magnetic disturbance compensation

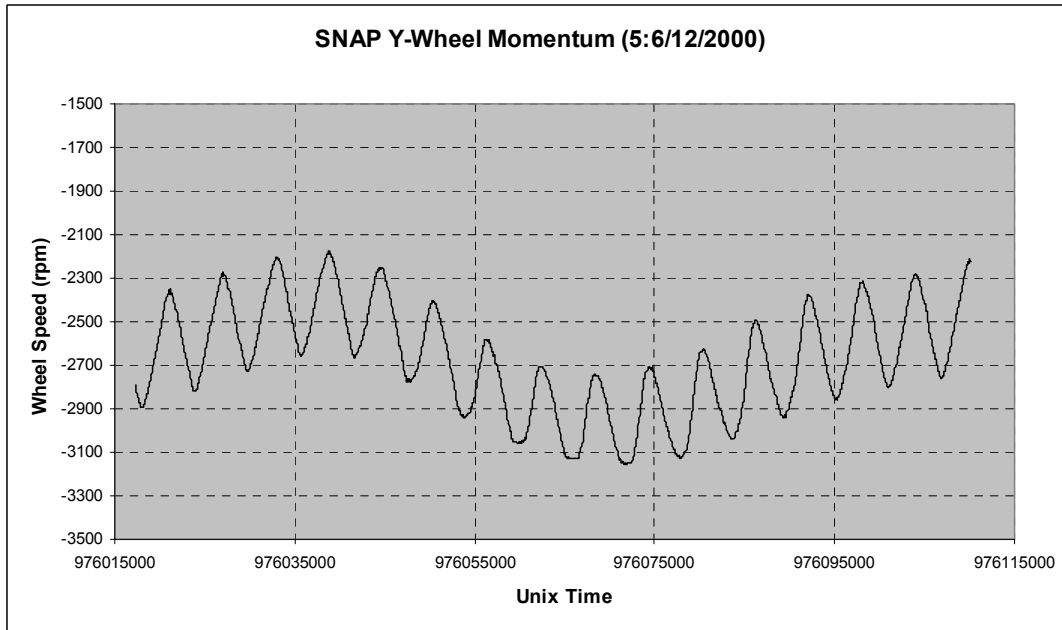


Figure 4: Initial Y-wheel performance with magnetic disturbance compensation

**Disturbance Estimation**

Suppose SNAP-1 is under the influence of an unknown permanent magnetic moment  $\mathbf{M}_d$ , the attitude equation can then be written as,

$$\mathbf{I}\dot{\boldsymbol{\omega}} = \boldsymbol{\Psi}\mathbf{M}_d + \mathbf{N} - \boldsymbol{\omega} \times (\mathbf{I}\boldsymbol{\omega} + \mathbf{h}) - \dot{\mathbf{h}} \quad (8)$$

with,

$\mathbf{N}$  is the external torque vector, mainly due to the known magnetorquer attitude control firings. The first term in the right hand-side of (8) is the

disturbance torque caused by SNAP-1’s magnetic moment and the matrix  $\boldsymbol{\Psi}$  is obtained by,

$$\boldsymbol{\Psi} = \begin{bmatrix} 0 & B_z & -B_y \\ -B_z & 0 & B_x \\ B_y & -B_x & 0 \end{bmatrix} \quad (9)$$

with,

$B_j$  is the vector component of Earth magnetic field measured by a magnetometer onboard. We assume that the magnetometer measurements are not

significantly disturbed by the disturbance magnetic moment.

If SNAP-1's angular body rate vector of  $\boldsymbol{\omega}$  is observable, we can design an estimator to evaluate the unknown  $\mathbf{M}_d$ . Let's define our state vector  $\mathbf{x}$  to be  $\boldsymbol{\omega}$  and  $\mathbf{M}_d$ , e.g.  $\mathbf{x} = [\boldsymbol{\omega} \ \mathbf{M}_d]^T$  and describe the system equation as:

$$\dot{\mathbf{x}} = \mathbf{f}(\mathbf{x}, t) + \mathbf{w} \quad (10)$$

with,

$\mathbf{w}$  = vector of system noise.

The system equation (10) for  $\boldsymbol{\omega}$  has already been shown in (8) and for  $\mathbf{M}_d$  a constant vector is assumed. From our measurement assumption, the observation matrix  $\mathbf{H}$  is,

$$\mathbf{H} = [\mathbf{I}_{3 \times 3} \ \mathbf{0}_{3 \times 3}] \quad (11)$$

As we conventionally do, the state transition matrix  $\Phi$  is approximated by,

$$\Phi \approx \mathbf{I}_{6 \times 6} + (\partial \mathbf{f} / \partial \mathbf{x}) \Delta t \quad (12)$$

Then we will be able to establish a recursive estimator by applying the standard formulae of a Kalman (or Extended Kalman) filter<sup>3</sup>.

Unfortunately, SNAP-1 does not have any rate sensors to measure the angular rate vector  $\boldsymbol{\omega}$ . We have decided to use the estimated  $\boldsymbol{\omega}$  from the onboard attitude estimator. The onboard attitude estimator estimates the attitude quaternion and the angular rate vector from the magnetometer measurements using a Kalman filter algorithm<sup>1</sup>.

Fundamentally this involves an iteration process until the estimated value of  $\mathbf{M}_d$  becomes stable. This value is now used in the onboard attitude estimator in order to take account of the disturbance

magnetic moment. We also intentionally decrease the measurement noise variance and increase the process noise variance slightly for the onboard estimator to rely more on the measurements and less on the dynamic model.

Figure 5 shows the result of the 1<sup>st</sup> estimation attempt of SNAP-1's unknown magnetic moment. The attitude log file on the 8<sup>th</sup> of February 2001 is used, which contains more than 1700 measurements sampled every 5 seconds. SNAP-1 was in a compass mode attitude on that day. This is because we intentionally stopped our Y-wheel closed loop pitch controller and the Y-wheel was kept running at a constant speed. The estimated magnetic moment value on the 1<sup>st</sup> attempt is:

(8/2/2001)

$$\mathbf{M}_d = [0.02 \ 0.04 \ -0.11]^T \text{ Am}^2 \quad (13)$$

In order to cancel the magnetic disturbance, we compensated the magnetorquer commands by biasing the firing times every 5 seconds as,

- 0.8 seconds for -X-firing pulse
- 1.6 seconds for -Y-firing pulse
- 4.4 seconds for +Z-firing pulse

In practice the Z-torquer can only be pulsed for 4 seconds maximum as already explained, so the attitude estimator must take into account the residual moment of  $-0.01 \text{ Am}^2$  in the Z-axis.

Consequently we did the iteration process using the SNAP-1 ADCS log file on the 14<sup>th</sup> and 27<sup>th</sup> of February 2001 and our final estimated magnetic moment is:

(27/2/2001)

$$\mathbf{M}_d = [0.034 \ 0.036 \ -0.12]^T \text{ Am}^2 \quad (14)$$

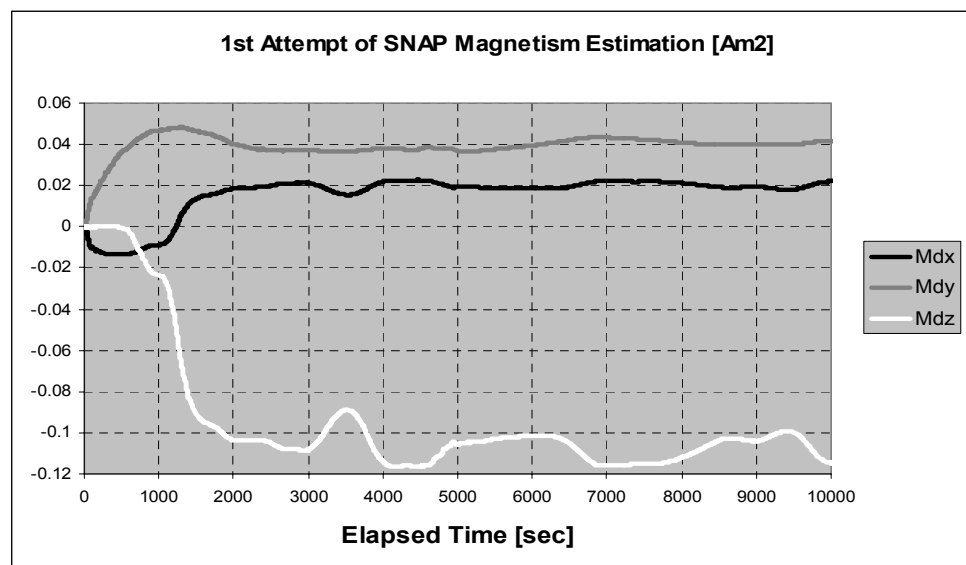
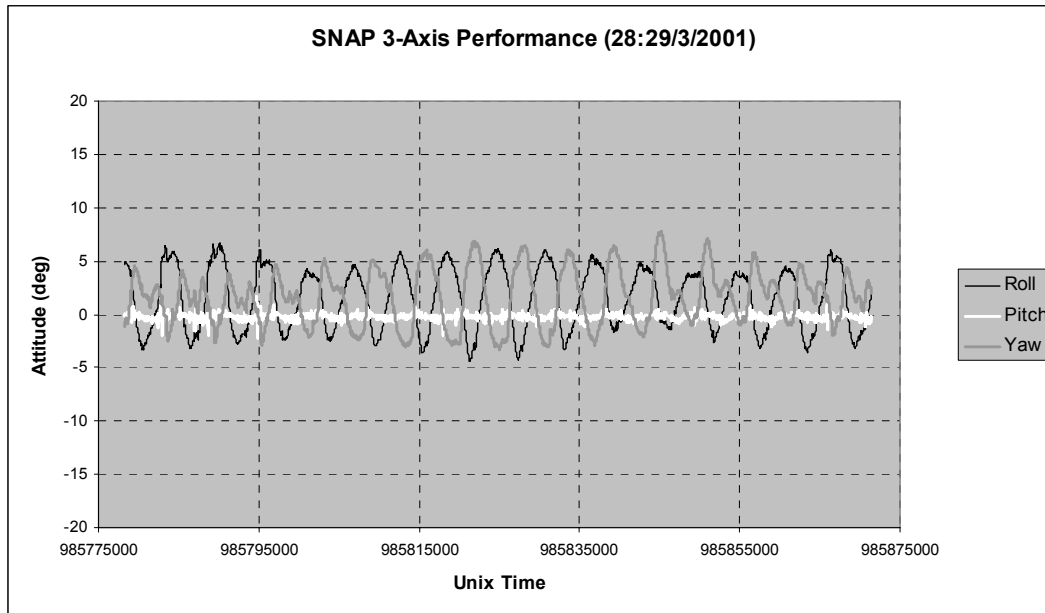


Figure 5: 1<sup>st</sup> Attempt (8/2/2001) of SNAP-1's magnetic moment estimation

### Final Performance

After several iterations of the magnetic moment estimator during magnetorquer compensation, the result of (14) was used to obtain the 3-axis stabilisation performance over a 28 hour period as shown in Figure 6. Table 5 compares the attitude performance before and after application of the disturbance estimator. It is clear from these graphs that we have managed to improve the cancellation of the disturbance magnetic moment significantly

above the initial attempts (Figures 3 and 4). The roll ( $1-\sigma$ ) variation has now been reduced to only  $2.9^\circ$  (about 25% of the previous result). The wheel momentum could be maintained closer to a speed of  $-2700$  rpm (see Figure 7) and only a  $\pm 100$  rpm variation once per orbit was needed to compensate for the residual magnetic disturbance torque in the Y-axis (7). The disturbance to the pitch axis attitude has also been reduced by almost an order of magnitude.



**Figure 6:** Final 3-Axis performance with magnetic disturbance compensation

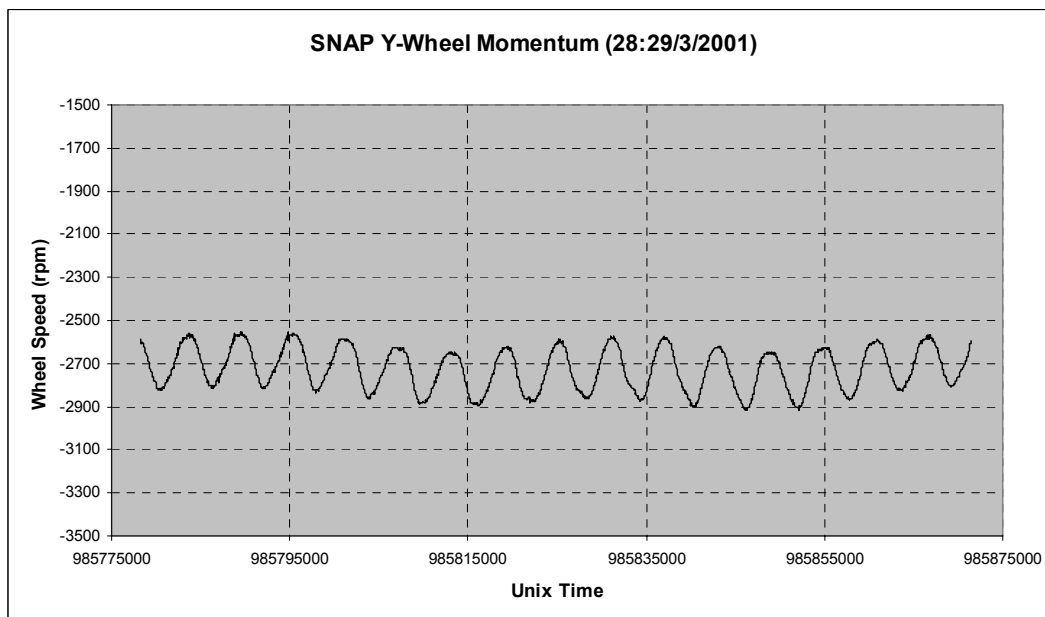


**Figure 7:** Final Y-wheel performance with magnetic disturbance compensation

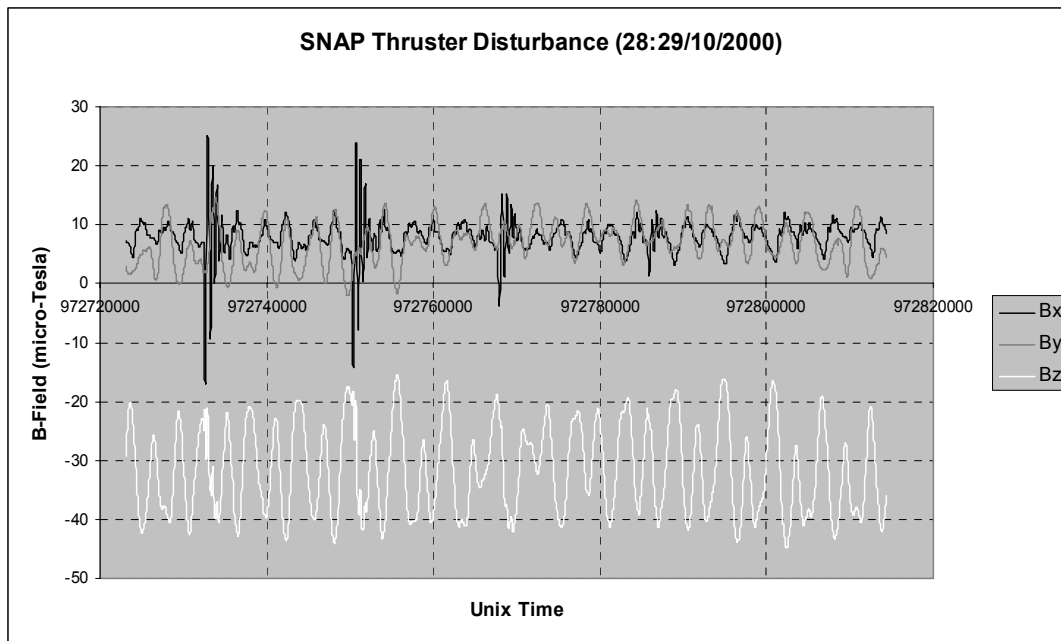
**Table 5:** Comparison of 3-axis stabilisation attitude performance

|                            | Avg.Roll | Avg.Pitch | Avg.Yaw | Roll (1- $\sigma$ ) | Pitch (1- $\sigma$ ) | Yaw (1- $\sigma$ ) |
|----------------------------|----------|-----------|---------|---------------------|----------------------|--------------------|
| <b>Initial @ 6/12/2000</b> | 1.6°     | -0.7°     | 1.6°    | 11.4°               | 2.0°                 | 6.6°               |
| <b>Final @ 29/3/2001</b>   | 1.5°     | -0.2°     | 1.6°    | 2.9°                | 0.3°                 | 2.6°               |

### Thruster Disturbances

All propulsion firings took place between August and October 2000, while SNAP-1 was controlled into a compass mode attitude. Initially the firings were done with only magnetorquers to damp the thruster disturbance caused by misalignment. All firings took place over the equatorial region during an ascending pass when the thrust vector (+Z-axis) was roughly anti-parallel to the velocity vector (to raise SNAP-1's semi-major axis). Later the Y-wheel was also used to supply a constant body momentum vector along the orbit anti-normal to improve the thrust vector alignment to the velocity vector.

Figure 8 shows the final attitude disturbances (as observed in the B-field measurements) on the 28<sup>th</sup> of October 2000, when the propulsion system ran out of fuel. A total of 5 firings (separated every 3 orbits) at decaying strength, can be seen. Each of these firings was 3 seconds in duration. From the attitude estimator the disturbance was mainly in the pitch axis (Y-axis). The peak pitch transient was about 55° during compass mode (see Figure 9). By using a full dynamic simulation of the compass mode attitude, the thruster disturbance torque was then estimated to be,  $N_{dy} = 0.19$  milli-Nm. If we assume an average thruster force of 50 milli-N, the misalignment along the Z-axis is about 4 mm.

**Figure 8:** Final thruster disturbances as observed by the B-field measurements while in compass mode

### Orbit Determination Results

We have demonstrated experimental orbit control using the butane thruster<sup>4</sup>. Our challenge was to rendezvous SNAP-1 with Tsinghua-1, at least within a range of a few hundred kilometres where we will be able to demonstrate our inter-satellite communication experiment.

Due to the separation sequence, from the very beginning we observed about 1.5 kilometres difference in the semi-major axis between the two satellites, with SNAP-1's semi-major axis lower than that of Tsinghua-1. As we expected, the orbital decay rate due to atmospheric drag is more significant for SNAP-1 than for Tsinghua-1, hence it was required to commence the experiment as soon as practical.

On the 15<sup>th</sup> of August 2000, we performed a successful butane thruster firing test of only 0.1 seconds. At that stage, the separation angle between the two satellites was nearly 90° (a quarter of an orbit). After a few more performance tests of the thrusters, since the 30<sup>th</sup> of August 2000, we started routinely to fire the butane thruster for 3 seconds every 3 to 4 orbits. Around the 11<sup>th</sup> of September 2000, we met the peak separation angle of approximately 124° (one third of an orbit), at which time SNAP-1's semi-major axis almost caught up with Tsinghua-1's.

We stopped the orbit manoeuvring on the 19<sup>th</sup> of September 2000, when SNAP-1's semi-major axis was at the target value of about 1 kilometre higher than that of Tsinghua-1. We observed, however, the a faster decay of semi-major axis than expected, hence we re-scheduled the firings to raise the semi-major axis again since the 20<sup>th</sup> of October 2000 and noticed that we consumed all SNAP-1's butane fuel on the 28<sup>th</sup> of October 2000. According to our prediction, if the drag effect would become weaker, there could still be a possibility to demonstrate a rendezvous between the two satellites. However, if not, we might miss the opportunity for any close approach between the two satellites. Unfortunately, the closest approach of the two satellites happen around the 12<sup>th</sup> of March 2000 with a separation angle of 16.7° (approximately still 2000 kilometres

away), which was one order of magnitude bigger than our original target.

Throughout these orbit control sequence, SNAP-1's orbit was determined by a ground based epicycle orbit estimator<sup>5</sup>, using downloaded onboard GPS measurements (we are using the GPS navigation solution as the measurement). The GPS receiver, a SGR-05<sup>6</sup>, is manufactured by SSTL to be used specifically on our nanosatellites (see Table 1). Due to power budget reasons, we obtained GPS measurements for 3 to 4 orbits per day, sampled every 20 seconds.

The history of SNAP-1's semi-major axis and eccentricity during the orbit control experiment are shown in Figures 10 and 11. In Figure 10 we can clearly see the effect of the thruster firings and consequently the orbital decay on the semi-major axis due to atmospheric drag.

The long periodic variation we can be seen in the eccentricity profile (Figure 11), due to the  $J_3$  and  $J_2$  coupling effect. The period observed is the same as the period of the argument of perigee precession due to  $J_2$  (approximately 115 days for SNAP-1's orbit).

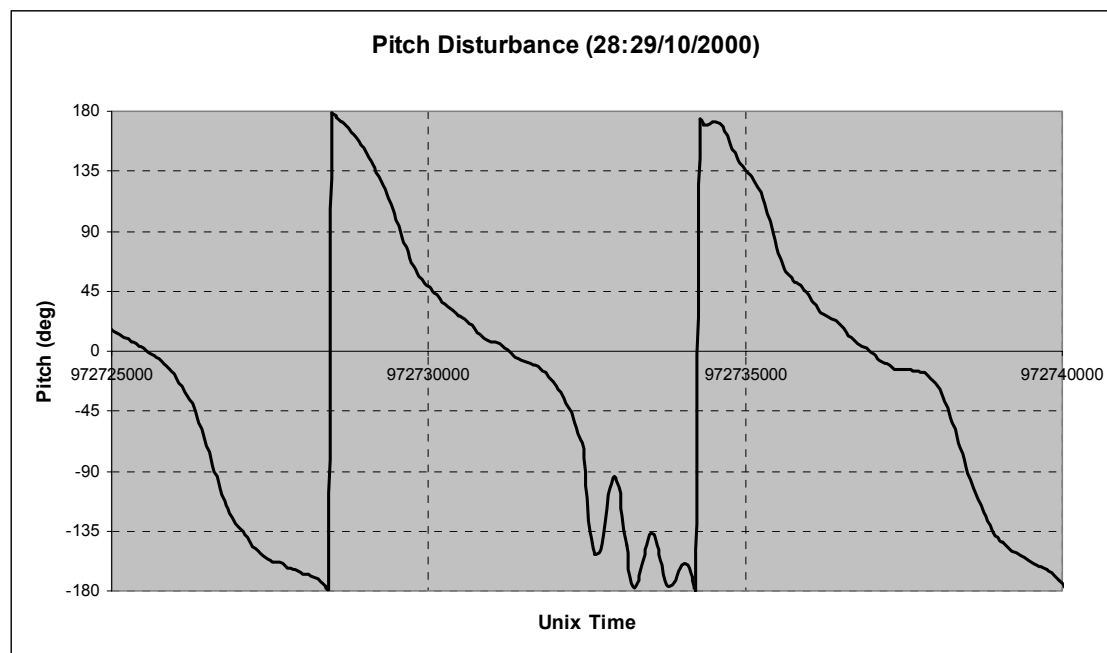


**Figure 9:** SNAP-1's Pitch attitude disturbance during thruster firings



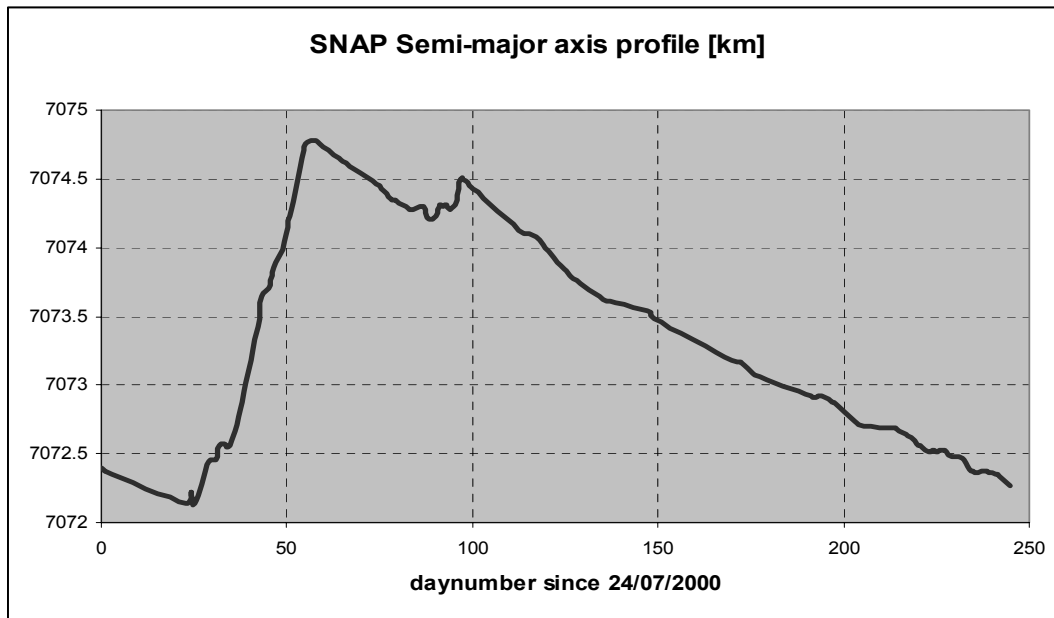


**Figure 10:** SNAP-1's Semi-major axis history during the Orbit Control Experiment

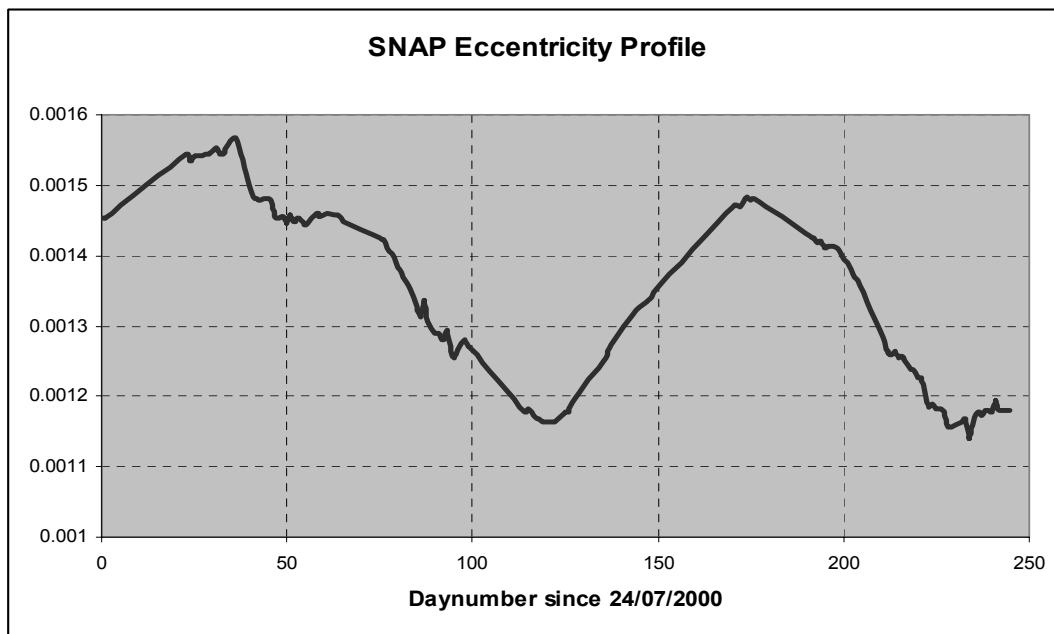


**Figure 11:** SNAP-1's Eccentricity history during the Orbit Control Experiment

### Conclusions

Successful 3-axis nadir pointing stabilisation has been demonstrated on SNAP-1, using a minimum set of sensors and actuators. However, a problem caused by a large internal magnetic moment disturbance had to be solved first. Several weeks of effort was spent to characterise the disturbance and then to partially cancel it using the

magnetorquer rods, still resulting in unsatisfactory 3-axis nadir pointing performance.

It was realised that both the Y-wheel dynamics and the magnetic moment cross coupling influence, caused by the magnetorquer rods, complicated an accurate estimation of the internal disturbance. A new in-situ (with active magnetorquer compensation) magnetic moment estimator was developed

and after a few iterations, we have managed to reduce the 3-axis attitude stability to acceptable levels. The current nadir pointing performance is within  $3^\circ$  ( $1-\sigma$ ) and the stability good enough for Earth imaging 24 hours per day.

The Y-momentum wheel stabilisation method will give good performance for a nadir pointing application, if the internal and external disturbance torques can be kept to small values. An internal magnetic moment disturbance can be compensated for, if accurately identified and within the capability of the magnetorquer rods.

Misalignment of the thrust vector to the centre of mass of the satellite can cause significant disturbances to the attitude. On SNAP-1 we have managed to characterise the thruster misalignment and the magnetorquers were capable to damp the resulting attitude disturbance within one orbit.

The orbit determination filter, using the GPS data from SNAP-1, enabled us to predict and plan all our orbit control manoeuvres. Although we were not able to demonstrate a rendezvous, we have gained useful experience and also performed the first nanosatellite orbit control demonstration, using the butane thruster under ADCS support.

The authors wish to thank the SNAP-1 team at the Surrey Space Centre for all the support and the continuing success of the SNAP nanosatellite mission after more than 1 year in orbit.

## References

1. Steyn, W.H., Hashida Y. and Lappas V., "An Attitude Control System and Commissioning Results of the SNAP-1 Nanosatellite", Proceedings of the 14<sup>th</sup> Annual AIAA/USU Conference on Small Satellites, Utah State University, August 2000, SSC00-VIII-8.
2. Gibbon, D., Ward J. and Kay N., "The Design, Development and Testing of a Propulsion System for the SNAP-1 Nanosatellite", Proceedings of the 14<sup>th</sup> Annual AIAA/USU Conference on Small Satellites, Utah State University, August 2000, SSC00-I-3.
3. Brown, R.G., & Hwang, P.Y.C., "Introduction to Random Signals and Applied Kalman Filtering", John Wiley, 1997.
4. Gibbon, D., & Underwood C, "Low Cost Butane Propulsion Systems for Small Spacecraft", to be published in Proceedings of the 15<sup>th</sup> Annual AIAA/USU Conference on Small Satellites, Utah State University, August 2001.
5. Hashida, Y., & Palmer, P. L., "Analytic Approach for Near Circular Orbit Determination", to be published in Proceedings of the AIAA GNC Conference, Montreal, Canada, August 2001.
6. Unwin, M. J., Palmer, P. L., Hashida, Y. & Underwood, C. I., "The SNAP-1 and Tsinghua-1 GPS Formation Flying Experiment", ION GPS 2000, Salt Lake City, September 2000.